ADAPTIVE CHIP-LEVEL DELAY–DOPPLER TRACKING FOR DSSS-BASED UNDERWATER ACOUSTIC PLATFORMS

Jie Wu[1], Huayong Yang[1]

[1] *The Southern Marine Science and Engineering Guangdong Laboratory Guangzhou. Guangzhou, China*

Abstract

High-rate delay and motion estimation is important for maneuvering underwater platforms using direct-sequence spread-spectrum signals. Conventional frame- or symbol-level estimators provide limited temporal resolution, while direct differentiation of noisy delay measurements amplifies velocity-estimation errors. This paper proposes an adaptive delay-Doppler tracking method based on chip-level DSSS correlation observations. Sliding correlation and three-point interpolation are used to obtain sub-sample delay measurements. A coarse frame-level Doppler estimate is first obtained from the synchronization signal, and the residual Doppler variation is then extracted from the phase differences between consecutive complex correlation peaks after removing the BPSK data-dependent phase. A constant-acceleration Kalman tracker is then developed to jointly estimate propagation delay, radial velocity, and acceleration. Its measurement covariance is adaptively adjusted according to the peak-to-sidelobe ratio and local peak curvature. Simulations show that the proposed method reduces the delay and velocity RMSE compared with a fixed-covariance Kalman filter. Results from a Songhua Lake experiment further demonstrate that the estimated radial velocity is consistent with the GPS-derived reference. The proposed method enables DSSS communication waveforms to provide high-update-rate motion estimates without an additional acoustic ranging signal.

Keywords: *underwater acoustic communication, direct-sequence spread spectrum, delay tracking, Doppler estimation, adaptive Kalman filtering, maneuvering platform.*

1. Introduction

Underwater acoustic communication systems deployed on autonomous underwater vehicles and mobile observation platforms are strongly affected by relative motion. Underwater acoustic channels are characterized by limited bandwidth, severe multipath propagation, and significant temporal variability [1]. Because of the low propagation speed of sound, platform motion introduces not only carrier-frequency shifts but also time scaling and continuously varying propagation delays. These effects are particularly significant for long-frame direct-sequence spread-spectrum (DSSS) signals [2].

DSSS waveforms have favorable correlation properties and can provide propagation-delay measurements in addition to communication capability. Conventional receivers generally estimate Doppler parameters from a synchronization sequence and compensate for the Doppler scaling over an entire signal frame [3]. Although such methods are computationally efficient, they may be insufficient when the platform velocity changes significantly within one frame.

Model-based approaches have been developed to track time-varying Doppler parameters. Kalman filtering has been applied to spread-spectrum underwater acoustic systems to track symbol-level Doppler variations [4]. Per-survivor processing jointly estimates the transmitted symbols and channel parameters [5]. Iterative DSSS receivers have also been developed for channels with time-varying Doppler shifts [6]. In addition, line-of-sight peak detection and tracking can improve the stability of DSSS reception in doubly spread channels [7]. However, most existing methods update the motion parameters once per frame or spreading symbol. Moreover, the reliability of successive correlation peaks varies with noise, Doppler mismatch, and multipath interference, but this variation is rarely incorporated into the measurement covariance. Therefore, generating dense intra-frame observations and incorporating their time-varying reliability into motion tracking remain insufficiently investigated for maneuvering DSSS systems.

Our previous work focused on time-varying waveform reconstruction, amplitude-phase information utilization, and communication-performance improvement

Corresponding author: *wu_jie@gmlab.ac.cn.*

[8]. In contrast, this paper concentrates on high-rate motion estimation from chip-level DSSS correlation observations.

The main contributions are summarized as follows:

1. Chip-level delay observations and phase-based Doppler observations are jointly extracted from complex DSSS correlation peaks.

2. A peak-quality-aware Kalman tracker is developed by empirically mapping the peak-to-sidelobe ratio and local curvature to an adaptive measurement covariance.

2. Proposed Method

2.1. Signal and delay observation

The transmitted complex baseband DSSS signal is expressed as

$$x(t) = \sum_{m=0}^{N_s-1} b_m \sum_{l=0}^{L-1} c_l g\left(t - mT_s - lT_c\right), \tag{1}$$

where b_m denotes the modulated symbol, c_l is the spreading code, T_c is the chip interval, L is the spreading-code length, and $T_s = LT_c$ is the spreading-symbol interval. After coarse synchronization and Doppler compensation, the locally extracted dominant path is modeled as

$$y(t) = \alpha(t) x\left(t - \tau(t)\right) \exp\left[j2\pi \int_0^t f_D(\xi)\,\mathrm{d}\xi\right] + w(t), \tag{2}$$

where $\tau(t)$ and $f_D(t)$ denote the time-varying propagation delay and residual Doppler frequency, respectively. A sliding correlation is performed as

$$C_k(\ell) = \sum_{n=0}^{N_w-1} y[n + kD]\, s_k^*[n - \ell], \tag{3}$$

where N_w is the correlation-window length, D is the observation step in samples, and $s_k[n]$ is the local reference signal. The correlation window contains one complete spreading symbol and is shifted by one chip interval between consecutive observations. Therefore, adjacent observations are temporally correlated because their correlation windows overlap. The observation interval is $\Delta T = D/f_s$. The integer peak position is

$$\hat{\ell}_k = \arg\max_{\ell \in \Omega_k} \left|C_k(\ell)\right|, \tag{4}$$

where Ω_k is a local delay-search interval centered at the predicted dominant-path delay. Three-point parabolic interpolation is used to obtain the fractional peak offset

$$\delta_k = \frac{1}{2} \frac{r_{-1} - r_{+1}}{r_{-1} - 2r_0 + r_{+1}}, \tag{5}$$

where

$$\begin{aligned} r_{-1} &= \left|C_k\left(\hat{\ell}_k - 1\right)\right|, \\ r_0 &= \left|C_k\left(\hat{\ell}_k\right)\right|, \\ r_{+1} &= \left|C_k\left(\hat{\ell}_k + 1\right)\right|. \end{aligned} \tag{6}$$

The sub-sample delay observation is therefore

$$\hat{\tau}_k = \frac{\hat{\ell}_k + \delta_k}{f_s}. \tag{7}$$

2.2. Phase-based Doppler observation

The complex correlation peak at the interpolated position is written as

$$p_k = C_k\left(\hat{\ell}_k + \delta_k\right) = A_k \exp\left(j\phi_k\right). \tag{8}$$

For BPSK modulation, the square operation removes the data-dependent phase ambiguity because $b_k^2 = 1$. The residual Doppler observation is then calculated as

$$\hat{f}_{D,k} = \frac{1}{4\pi\Delta T} \angle \left[p_k^2 \left(p_{k-1}^*\right)^2\right], \tag{9}$$

where coarse Doppler compensation is performed beforehand so that the residual Doppler satisfies the unambiguous condition

$$|f_D| < \frac{1}{4\Delta T}. \tag{10}$$

Positive radial velocity is defined as increasing transmitter–receiver range. The corresponding velocity observation is

$$\hat{v}_{D,k} = -\frac{c}{f_c} \hat{f}_{D,k}, \tag{11}$$

where c is the sound speed and f_c is the carrier frequency. The delay measurement provides a stable range-related observation, whereas the Doppler measurement is more sensitive to rapid velocity changes.

2.3. Adaptive Kalman tracking

The state vector is defined as

$$\mathbf{x}_k = \begin{bmatrix} \tau_k & v_k & a_k \end{bmatrix}^{\mathrm{T}}. \tag{12}$$

The state-space formulation follows the classical Kalman-filtering and target-tracking framework [9], [10]. Using a constant-acceleration model,

$$\mathbf{x}_{k+1} = \mathbf{F}\mathbf{x}_k + \mathbf{w}_k, \tag{13}$$

with

$$\mathbf{F} = \begin{bmatrix} 1 & \frac{\Delta T}{c} & \frac{\Delta T^2}{2c} \\ 0 & 1 & \Delta T \\ 0 & 0 & 1 \end{bmatrix}. \tag{14}$$

The unmodeled variation of acceleration is represented by a piecewise-constant jerk process. Let

$j_k \sim \mathcal{N}(0, \sigma_j^2)$ and

$$\mathbf{w}_k = \mathbf{G} j_k, \qquad \mathbf{G} = \begin{bmatrix} \dfrac{\Delta T^3}{6c} \\ \dfrac{\Delta T^2}{2} \\ \Delta T \end{bmatrix}. \tag{15}$$

The process-noise covariance is

$$\mathbf{Q} = \mathbb{E}\left[\mathbf{w}_k \mathbf{w}_k^{\mathrm{T}}\right] = \sigma_j^2 \mathbf{G}\mathbf{G}^{\mathrm{T}}. \tag{16}$$

The observation model is

$$\mathbf{z}_k = \begin{bmatrix} \hat{\tau}_k \\ \hat{f}_{D,k} \end{bmatrix} = \mathbf{H}\mathbf{x}_k + \mathbf{n}_k, \tag{17}$$

where

$$\mathbf{H} = \begin{bmatrix} 1 & 0 & 0 \\ 0 & -\dfrac{f_c}{c} & 0 \end{bmatrix}. \tag{18}$$

To describe the reliability of the correlation peak, the peak-to-sidelobe ratio is defined as

$$\mathrm{PSR}_k = \frac{\left| C_k\left(\hat{\ell}_k\right) \right|}{\sqrt{\dfrac{1}{N_\Omega} \sum_{\ell \in \bar{\Omega}_k} \left| C_k(\ell) \right|^2 + \varepsilon}}, \tag{19}$$

where $\bar{\Omega}_k$ is the sidelobe region after excluding a guard interval around the dominant peak, and N_Ω is the number of samples in this region. The normalized peak curvature is

$$\kappa_k = \frac{2r_0 - r_{-1} - r_{+1}}{r_0 + \varepsilon}. \tag{20}$$

Because κ_k may become non-positive when the peak is strongly distorted, the effective delay- and Doppler-quality factors are defined as

$$q_{\tau,k} = \max\left[\mathrm{PSR}_k \max(\kappa_k, 0), q_{\min}\right], \tag{21}$$

and

$$q_{f,k} = \max\left[\sqrt{\mathrm{PSR}_k \mathrm{PSR}_{k-1}}, q_{\min}\right]. \tag{22}$$

The adaptive measurement variances are

$$\sigma_{\tau,k}^2 = \mathrm{clip}\left(\frac{\beta_\tau}{q_{\tau,k}}, \sigma_{\tau,\min}^2, \sigma_{\tau,\max}^2\right), \tag{23}$$

and

$$\sigma_{f,k}^2 = \mathrm{clip}\left(\frac{\beta_f}{q_{f,k}}, \sigma_{f,\min}^2, \sigma_{f,\max}^2\right), \tag{24}$$

where $\mathrm{clip}(x, x_{\min}, x_{\max}) = \min[\max(x, x_{\min}), x_{\max}]$. The measurement covariance is finally given by

$$\mathbf{R}_k = \mathrm{diag}\left(\sigma_{\tau,k}^2, \sigma_{f,k}^2\right). \tag{25}$$

The filter is initialized as

$$\hat{\mathbf{x}}_{0|0} = \begin{bmatrix} \hat{\tau}_1 & -\dfrac{c}{f_c}\hat{f}_{D,1} & 0 \end{bmatrix}^{\mathrm{T}}, \tag{26}$$

with

$$\mathbf{P}_{0|0} = \mathrm{diag}\left[\sigma_{\tau,1}^2, \left(\frac{c}{f_c}\right)^2 \sigma_{f,1}^2, \sigma_{a,0}^2\right]. \tag{27}$$

When the correlation peak is sharp and clearly separated from the sidelobes, the quality factors increase, resulting in smaller measurement variances. The filter consequently assigns a larger weight to the observations. When the peak is weak, broadened, or distorted, the measurement variances increase and the filter relies more strongly on the state prediction.

For a fair comparison, the fixed-covariance Kalman filter uses the same state model, process covariance, initialization, and observations as the proposed method. Its measurement covariance is fixed using the median values obtained from a calibration dataset:

$$\mathbf{R}_{\text{fixed}} = \mathrm{diag}\left[\mathrm{median}_k\left(\sigma_{\tau,k}^2\right), \mathrm{median}_k\left(\sigma_{f,k}^2\right)\right]. \tag{28}$$

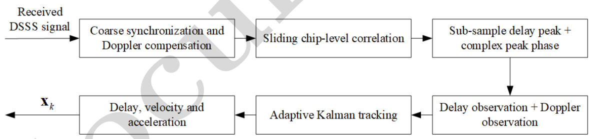

Figure 1: Processing flow of the proposed adaptive delay–Doppler tracking method.

3. Simulation Results

The simulated acoustic waveform uses the same carrier frequency, bandwidth, spreading sequence, modulation, and frame duration as the Songhua Lake experiment. A higher sampling frequency is used in the simulation to support sub-sample interpolation. The principal parameters are listed in Table 1.

Table 1: Simulation parameters.

Parameter	Value
Carrier frequency f_c	25 kHz
Bandwidth B	5 kHz
Simulation sampling frequency f_s	400 kHz
Chip interval T_c	0.2 ms
Spreading sequence	Kasami
Code length L	255
Modulation	BPSK
Frame duration	10 s
Observation step	One chip
Sound speed c	1500 m/s
Monte Carlo trials	500

The fixed-covariance Kalman filter and the proposed adaptive delay–Doppler Kalman filter are compared under identical signal, noise, state-model, and initialization conditions.

3.1. Validation under Idealized Dynamic Conditions

Two motion scenarios are first considered: a constant-velocity condition with $v = 10$ m/s and a constant-acceleration condition with $v_0 = 0$ m/s and $a = 3$ m/s^2. The first 2500 chip-level observations are used to illustrate the transient tracking performance. The delay and velocity estimates converge after approximately 300-500 chip observations. The remaining delay fluctuation is approximately 0.04 μs. Under the constant-acceleration condition, the absolute velocity-estimation error decreases to approximately 0.001 m/s after about 500 chip observations. These values are used only to verify the state model under ideal conditions and should not be interpreted as practical accuracy in a multipath lake channel.

3.2. Estimation Performance under Varying SNR Conditions

Additive white Gaussian noise is added, and the input SNR varies from −15 to 5 dB. For each SNR, 500 independent Monte Carlo trials are conducted. The evaluation metrics are

$$\mathrm{RMSE}_\tau = \sqrt{\frac{1}{K}\sum_{k=1}^{K}(\hat{\tau}_k - \tau_k)^2}, \tag{29}$$

and

$$\mathrm{RMSE}_v = \sqrt{\frac{1}{K}\sum_{k=1}^{K}(\hat{v}_k - v_k)^2}. \tag{30}$$

The fixed-covariance Kalman filter provides smooth estimates but cannot adapt its measurement weighting when the correlation-peak quality changes. In contrast, the proposed method increases the observation covariance for weak or distorted peaks and decreases it for reliable peaks. As shown in Fig. 3, the proposed method achieves a lower velocity RMSE over the investigated SNR range, particularly after the correlation peak becomes reliably detectable. The pronounced transition in the RMSE curve reflects the acquisition threshold of the chip-level correlation observations.

4. Lake Experiment and Results

A lake experiment was conducted on October 24, 2021, in Songhua Lake, Jilin City, China. Two vessels were used, with one vessel drifting freely and the other navigating continuously. The transmitting and receiving transducers were both deployed at a depth of approximately 1.8 m. A continuously transmitted Kasami-coded DSSS waveform was employed, with a carrier frequency of 25 kHz, a bandwidth of 5 kHz, and a frame duration of 10 s.

Figure 4 presents the delay–time correlation map of the continuously received DSSS signals. A dominant path with a continuously varying delay is visible throughout the observation interval, together with weaker time-varying multipath components. The curved dominant-path trajectory indicates substantial variation of the propagation delay caused by the relative motion between the two vessels. The measured channel therefore provides a representative dynamic environment for evaluating the proposed tracker.

The chip-level observations are then processed using the proposed method. Figure 5 compares the estimated radial velocity with the GPS-derived reference. The GPS positions of both vessels are converted into the relative radial velocity along the instantaneous transmitter–receiver line of sight and interpolated to the acoustic observation time stamps. The proposed method follows the overall increase and subsequent decrease of the relative radial velocity over the complete observation interval. The enlarged interval also shows that the acoustic estimate reproduces short-term velocity variations. The remaining differences may arise from acoustic measurement noise, imperfect time alignment, and the different update rates of the acoustic and GPS measurements.

To assess the noise robustness using measured data, additive white Gaussian noise is added to the lake-trial waveform to generate different input SNRs. The delay trajectory extracted from the original unperturbed waveform is used as a common reference for both methods. Figure 6 compares the delay-estimation RMSE of the fixed-covariance Kalman filter and the proposed method. The adaptive method achieves a lower RMSE over the investigated SNR range because it reduces the contribution of weak or distorted correlation peaks. As the input SNR increases, both methods approach their interpolation and sampling error floors, while the proposed method maintains the lower error floor.

5. Conclusion

This paper proposed an adaptive delay–Doppler tracking method based on chip-level DSSS correlation observations. Sub-sample delay measurements were obtained using sliding correlation and three-point interpolation, while residual Doppler was extracted from the phase evolution of consecutive complex correlation peaks. A peak-quality-aware measurement covariance was introduced into a constant-acceleration Kalman tracker to jointly estimate delay, radial velocity, and acceleration.

The simulations used the same 25 kHz carrier frequency and 5 kHz bandwidth as the Songhua Lake experiment. The proposed method achieved lower delay- and velocity-estimation RMSE than the fixed-covariance Kalman filter. The lake-trial results further showed that the estimated radial velocity followed the GPS-derived reference in a time-varying multipath channel. These results indicate that DSSS communication signals can provide high-rate motion measurements without an additional ranging waveform.

Future work will address the temporal correlation between overlapping chip-level observations, multipath-induced peak switching, and sea-trial validation under lower-SNR and intermittent direct-path conditions.

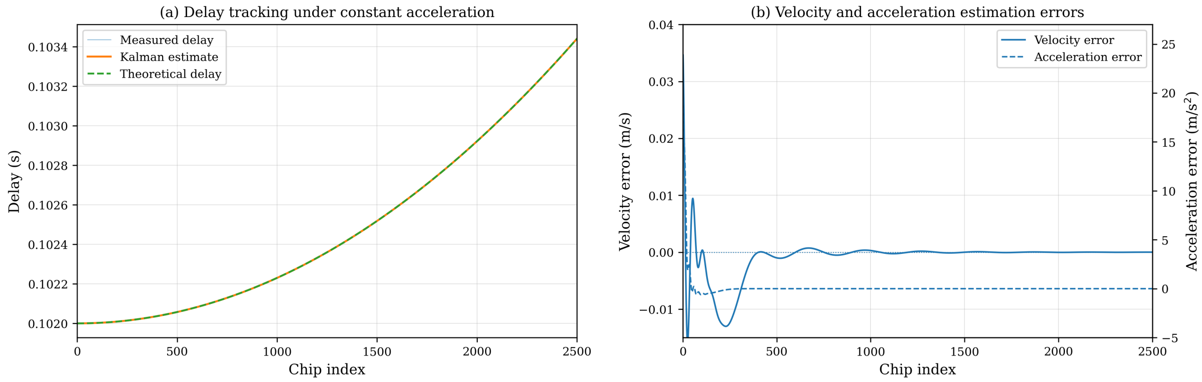

Figure 2: Tracking performance under the constant-acceleration condition: (a) measured, theoretical, and Kalman-filtered delays; (b) velocity- and acceleration-estimation errors.

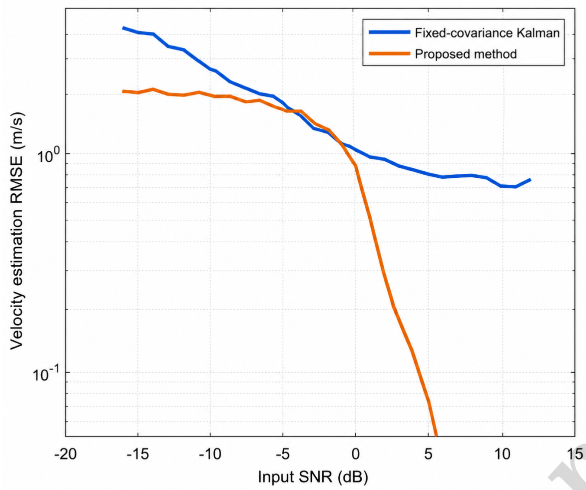

Figure 3: Velocity-estimation RMSE versus input SNR.

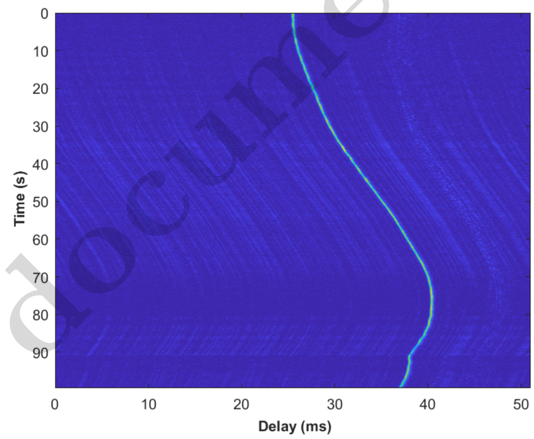

Figure 4: Delay–time correlation map of the continuously transmitted Kasami-coded DSSS signal in the Songhua Lake experiment.

6. Acknowledgments

This work was supported by the National Key Research and Development Program of China under Grant 2025YFE0214800, and the China Postdoctoral Science Foundation under Grant Number 2025M780261.

References

[1] M. Stojanovic and J. Preisig, "Underwater acoustic communication channels: Propagation models and statistical characterization," *IEEE Commun. Mag.*, vol. 47, no. 1, pp. 84–89, Jan. 2009. DOI: `10.1109/MCOM.2009.4752682`.

[2] C. Liu, Y. V. Zakharov, and T. Chen, "Doubly selective underwater acoustic channel model for a moving transmitter/receiver," *IEEE Trans. Veh. Technol.*, vol. 61, no. 3, pp. 938–950, Mar. 2012. DOI: `10.1109/TVT.2012.2187226`.

[3] B. S. Sharif, J. Neasham, O. R. Hinton, and A. E. Adams, "A computationally efficient Doppler compensation system for underwater acoustic communications," *IEEE J. Ocean. Eng.*, vol. 25, no. 1, pp. 52–61, Jan. 2000. DOI: `10.1109/48.820736`.

[4] D. Sun, X. Hong, and H. Cui, "A Kalman-based Doppler tracking algorithm for underwater acoustic spread spectrum communications," *Appl. Acoust.*, vol. 185, 108374, Jan. 2022. DOI: `10.1016/j.apacoust.2021.108374`.

[5] X. Xu, S. Zhou, A. K. Morozov, and J. C. Preisig, "Per-survivor processing for underwater acoustic communications with direct-sequence spread spectrum," *J. Acoust. Soc. Am.*, vol. 133, no. 5, pp. 2746–2754, May 2013. DOI: `10.1121/1.4796130`.

[6] D. Sun, J. Wu, X. Hong, C. Liu, H. Cui, and B. Si, "Iterative double-differential direct-sequence spread spectrum reception in underwater acoustic channel with time-varying Doppler shifts," *J. Acoust. Soc. Am.*, vol. 153, no. 2, pp. 1027–1041, Feb. 2023. DOI: `10.1121/10.0017116`.

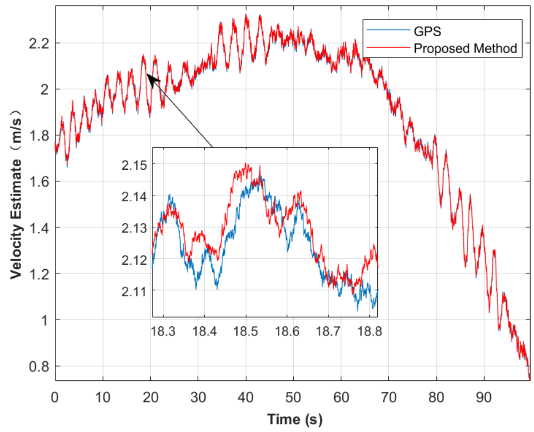

Figure 5: Comparison between the GPS-derived relative radial velocity and the velocity estimated by the proposed method. The inset shows an enlarged view of a representative interval.

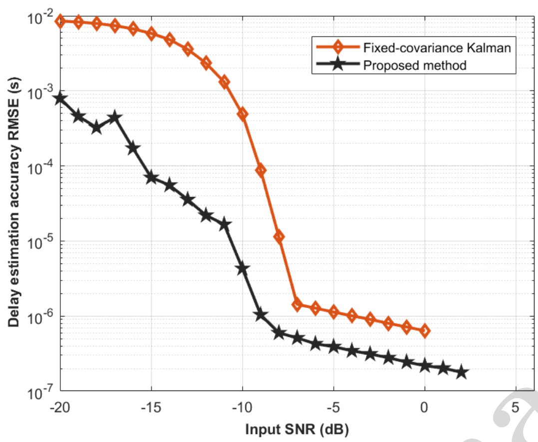

Figure 6: Delay-estimation RMSE versus input SNR for the fixed-covariance Kalman filter and the proposed method using the measured lake-trial waveform.

[7] D. Sun, J. Wu, H. Cui, Y. Fu, X. Hong, and C. Zheng, "The line-of-sight peak detection and tracking of underwater acoustic DSSS communications in the doubly spread channel," *Appl. Acoust.*, vol. 216, 109761, Jan. 2024. DOI: 10.1016/j.apacoust.2023.109761.

[8] J. Wu, C. Fa, S. Cang, and H. Yang, "A robust technique for joint parameter estimation with integrated communication and measurement in time-varying underwater acoustic channels," in *Proc. 2025 8th Int. Conf. Inf. Commun. Signal Process. (ICICSP)*, IEEE, 2025, pp. 310–314. DOI: 10.1109/ICICSP66564.2025.11338268.

[9] R. E. Kalman, "A new approach to linear filtering and prediction problems," *J. Basic Eng.*, vol. 82, no. 1, pp. 35–45, Mar. 1960. DOI: 10.1115/1.3662552.

[10] Y. Bar-Shalom, X. R. Li, and T. Kirubarajan, *Estimation with Applications to Tracking and Navigation: Theory, Algorithms, and Software*. New York, NY, USA: Wiley, 2001, ISBN: 9780471416555.